minerals

MDPI

Article

Anion Composition of Apatite in the Au-Cu Epithermal Deposit of Palai-Islica (Almería, SE Spain) as an Indicator of Hydrothermal Alteration

Javier Carrillo-Rosúa [1,2], Iñaki Esteban-Arispe [3] and Salvador Morales-Ruano [2,4,*]

1 Departamento de Didáctica de las Ciencias Experimentales, Universidad de Granada, Campus Universitario de Cartuja, 18071 Granada, Spain; fjcarril@ugr.es
2 Instituto Andaluz de Ciencias de la Tierra, Universidad de Granada—C.S.I.C., Avenida Las Palmeras 4, 18100 Armilla, Spain
3 Trail Ingenieros, Calle Ibáñez de Bilbao, 13. Entresuelo Derecha, 48009 Bilbao, Spain; iesteban@trailingenieros.com
4 Departamento de Mineralogía y Petrología, Universidad de Granada, Avenida Fuentenueva s/n, 18002 Granada, Spain
* Correspondence: smorales@ugr.es

Abstract: The Palai-Islica deposit (Almería, SE Spain) is an Au-Cu epithermal deposit hosted in Neogene calc-alkaline andesites and dacites from the Cabo de Gata-Cartagena volcanic belt in the Betic Cordillera. Major element compositions of apatite from Palai-Islica orebody and related hydrothermally altered and unaltered volcanic rock from the region hosting the deposit were obtained to clarify the processes involved in their formation. Apatite in the host volcanic rocks is rich in chlorapatite and hydroxylapatite components (50–57% and 24–36%) and poor in fluorapatite components (12–21%), indicating assimilation processes of cortical Cl-rich material in the magmatic evolution. Apatite in the orebody sometimes has corrosion textures and is mostly fluorapatite (94–100%). Apatite from the hydrothermally altered host rock of the orebody systematically bears signs of corrosion and has variable and intermediate fluorapatite (19–100%), chlorapatite (1–50%), and hydroxylapatite (0–47%) components. The style of zonation and the composition are related to the proximity to the orebody. These features can be interpreted as the result of hydrothermal modification of high Cl, OH-rich volcanic apatites into F-rich apatites. The enrichment of F is related to the intensity of hydrothermal alteration and could therefore constitute a geochemical index of alteration and of mineralization processes.

Keywords: apatite; epithermal deposits; hydrothermal alteration; mineral chemistry; Spain

Citation: Carrillo-Rosúa, J.; Esteban-Arispe, I.; Morales-Ruano, S. Anion Composition of Apatite in the Au-Cu Epithermal Deposit of Palai-Islica (Almería, SE Spain) as an Indicator of Hydrothermal Alteration. *Minerals* **2021**, *11*, 1358. https://doi.org/10.3390/min11121358

Academic Editors: Antonia Cepedal and Mercedes Fuertes-Fuente

Received: 2 October 2021
Accepted: 25 November 2021
Published: 30 November 2021

1. Introduction

Apatite [$Ca_5(PO_4)_3(F,Cl,OH)$] is the most abundant phosphate in the Earth's crust and appears in very different geological environments. It is a very common accessory phase in igneous and metamorphic rocks. In sedimentary environments, it is the most abundant mineral in phosphorites produced by biological activity, appearing occasionally in detrital materials. Apatite is a highly interesting mineral for study due to the large range of information that it can supply, including petrogenetic conditions by trace element content, cooling ages by fission track, and chronometry of exhumation processes and erosion rates using (U-Th)/He spectrometry. Apatite presents great chemical variability regarding its anion content, with a wide range of solid solutions among the different end members (e.g., [1,2]). This chemical variability can provide highly significant information on the genetic conditions of the apatite. Nevertheless, it should be noted that, whereas the composition of the apatite is well characterized in magmatic rocks (e.g., [1,3–15]), and to a lower degree in hydrothermal apatites (e.g., [16–18]), or even as a provenance indicator (e.g., [19]), there is very little information specifically on epithermal deposits

(e.g., [20,21]). In this work, apatite from the epithermal deposit of Au-Cu of Palai-Islica (Almería, SE of Spain) has been characterized texturally and chemically. The aim of this study is to establish the chemical variability of apatite in a hydrothermal environment and, especially, to investigate the use of major-element content as an indicator of the intensity of the mineralization processes.

2. Geological and Mineralogical Features

The Cabo de Gata-Cartagena volcanic belt formed on top of the eastern end of the Internal Zone of the Betic Cordillera, the western segment of Alpine orogeny. This Neogene volcanic belt (ages ranging from 20.9 Ma to 6.2 Ma [22–24]), with calc-alkaline, potassic calc-alkaline, shoshonitic, ultra potassic, and basaltic series [25], was formed during the extension of a thickened lithosphere [23]. The calc-alkaline magmatism is much more voluminous than the other series and is the only one that hosts gold deposits: Rodalquilar [26], Cabo de Gata [27,28], and Palai-Islica [29] (Figure 1).

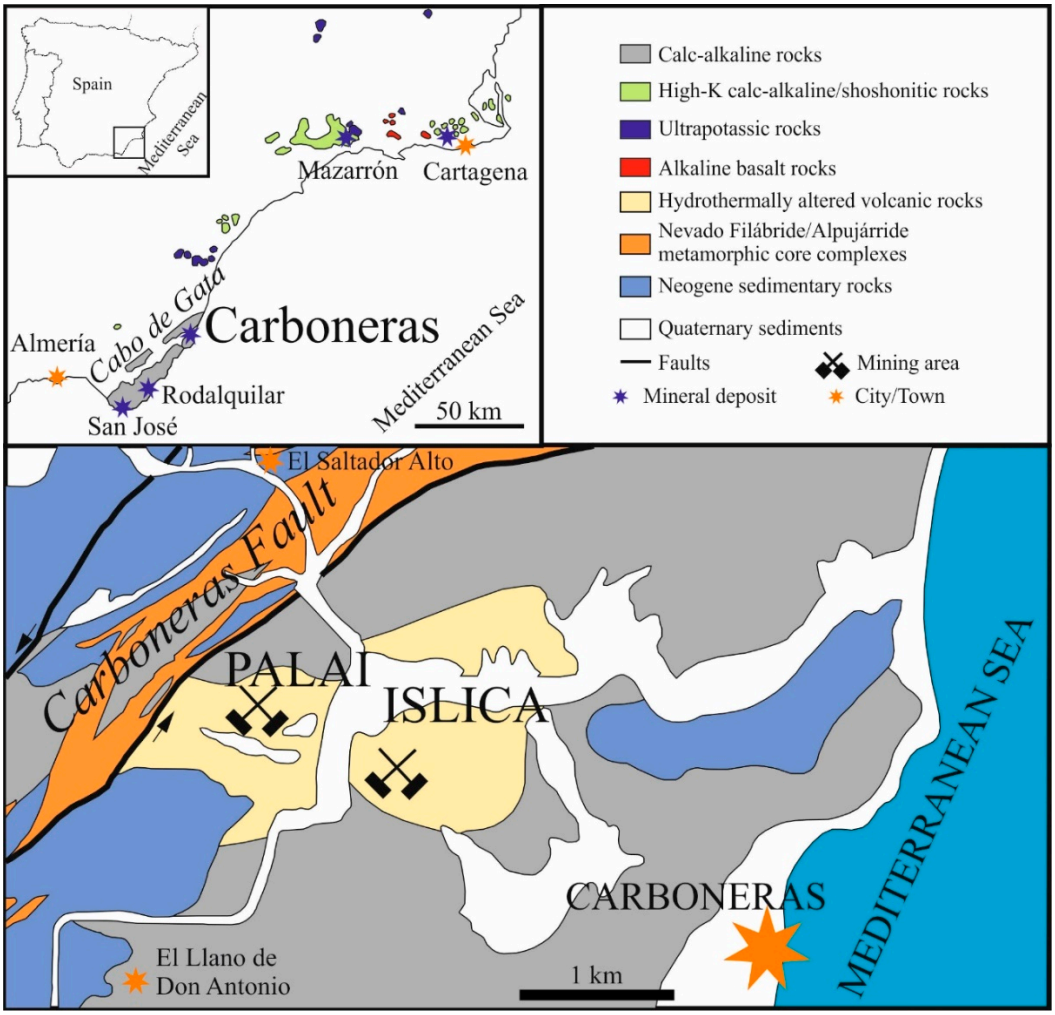

Figure 1. Simplified geological map of the Cabo de Gata–Cartagena volcanic province in SE of Spain (upper left) and of the Palai-Islica epithermal Au-Cu volcanic-hosted deposit (bottom). Adapted from [25,30,31].

The Palai-Islica deposit is located close to the town of Carboneras (Almería Province, Figure 1). In this area, four volcanic units (CB-1, CB-2, CB-3, and CB-4) have been described [32]. The CB-1 unit is defined by lava flows and autobreccias of andesite composition with pyroxene and amphibole. The CB-2 unit is defined by pyroclastic amphibolic dacite-andesites. The CB-3 unit shows the greatest thickness and extension. Finally, CB-4 is the last volcanic episode of the zone, defined by a dome formed by andesites with pyrox-

ene. The CB-1, CB-2, CB-3, and CB-4 units have K-Ar ages of 15.5–12.2 Ma, 10.7–10.9 Ma, 10.4 Ma, and 8.7 Ma, respectively [33].

The Palai-Islica deposit is hosted by andesite-dacite autobreccias with a domal structure from the CB-3 unit. These rocks are porphyritic with a high proportion of plagioclase and hornblende phenocrysts and lesser clino- and orthopyroxene and quartz phenocrysts. Biotite, apatite, magnetite, ilmenite, and zircon are also present in minor quantities [32]. These rocks are formed by multivent volcanic activity and developed in an intermediate-acid volcanic event [32]. Contemporary to late volcanism, an important hydrothermal system was developed in the zone associated with the mineralization.

The orebody consists of quartz veins with sulfides surrounded by andesite-dacites with sericitic-chloritic and propylitic alteration (Figure 2), as well as minor massive silicification with envelopes of argillic and advanced argillic alteration at the top of the deposit [29,34].

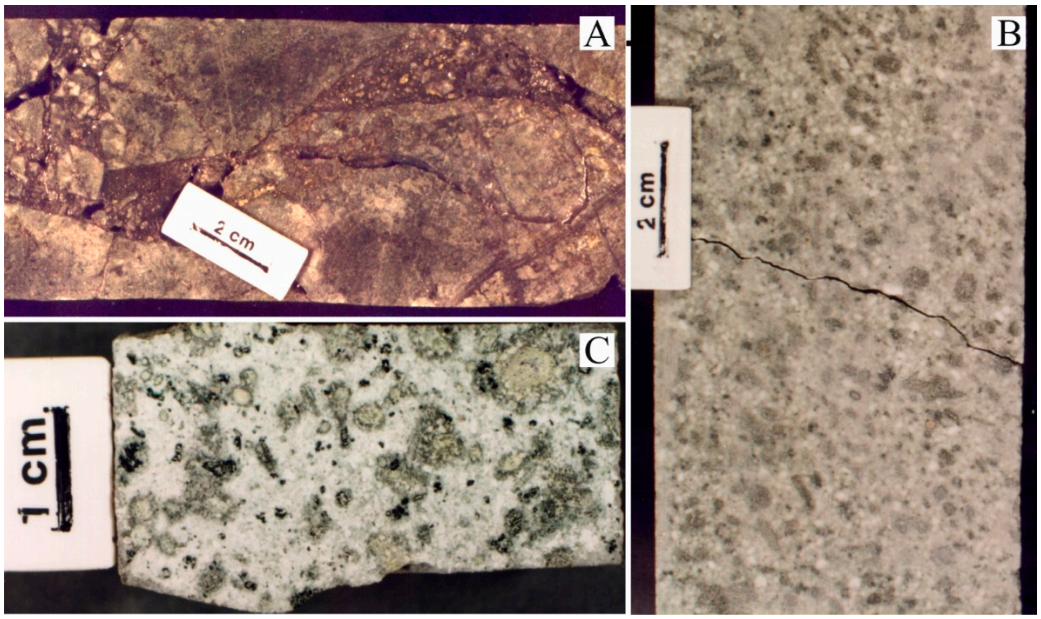

Figure 2. Hand-specimen samples from the Palai-Islica deposits containing some of the studied apatite crystals. (**A**) Mineralized veins and veinlets of quartz with sulfides. (**B**) Volcanic rock with sericitic-chloritic hydrothermal alteration mainly characterized by a transformation of phenocryst and groundmass to chlorite, muscovite, and quartz. (**C**) Volcanic rock with propylitic hydrothermal alteration characterized by a transformation of phenocryst and groundmass to chlorite, epidote, carbonates, and quartz.

The ore mineralogy consists of pyrite with lower amounts of chalcopyrite, sphalerite, and galena along with Au-Ag alloy, native gold, and a range of Ag sulfides and sulfosalts as precious metal-bearing minerals [35–37]. The gangue consists mainly of quartz, muscovite, and chlorite, with lesser barite, gypsum, and dolomite [38]. Apatite crystals are also found in small quantities in three different positions: within the orebody, within the hydrothermally altered host rocks with sericitic-chloritic and propylitic alteration, and in the unaltered host volcanic rocks (calc-alkaline andesite and dacite). Hydrothermal fluids deduced from fluid inclusion studies show temperatures between 118 and 453 °C and salinities ranging from 0.2 to 51.4 wt% NaCl eq. [29,39]. Isotopic constraints suggest a complex origin and evolution of hydrothermal fluids, with the involvement of magmatic and surface waters [39,40]. The deposit is an epithermal volcanic-hosted deposit in which high and intermediate sulfidation environments coexists in the same hydrothermal deposit [39], with the apatite only found in the latest one.

The most intense mineralization process took place in two subhorizontal levels, at around +45 m above sea level (masl), termed the Upper Geochemical Anomaly (UGA), and

–65 masl termed the Lower Geochemical Anomaly (LGA) and located in the intermediate sulfidation system. Both mineralized levels are characterized by concentrations of Au–Ag alloys and Ag-bearing phases, lithogeochemical positive anomalies in Au, Ag, Cu, and other metals, and fluid inclusions with distinct characteristics, especially highly variable salinity in a temperature range between 250–300 °C [29,35].

3. Textural and Chemical Characteristics of Apatite

Taking into account that apatite crystals are scarce, 14 samples, selected from around 250 samples from Palai-Islica deposit and surrounding area, have been studied. These samples belong to four different locations: (a) unaltered CB-3 volcanic rocks that host the orebody from the same unit far away from the deposit; (b) barren volcanic rocks from different units in the region (CB-1, CB-2, and CB-4 units); (c) mineralized zones; and (d) sericitic-chloritic and propylitic hydrothermal alteration. The apatite in the volcanic rocks appears as idiomorphic crystals (around a hundred μm in size) always included in maphic phenocrysts, such hornblende (Figure 3A).

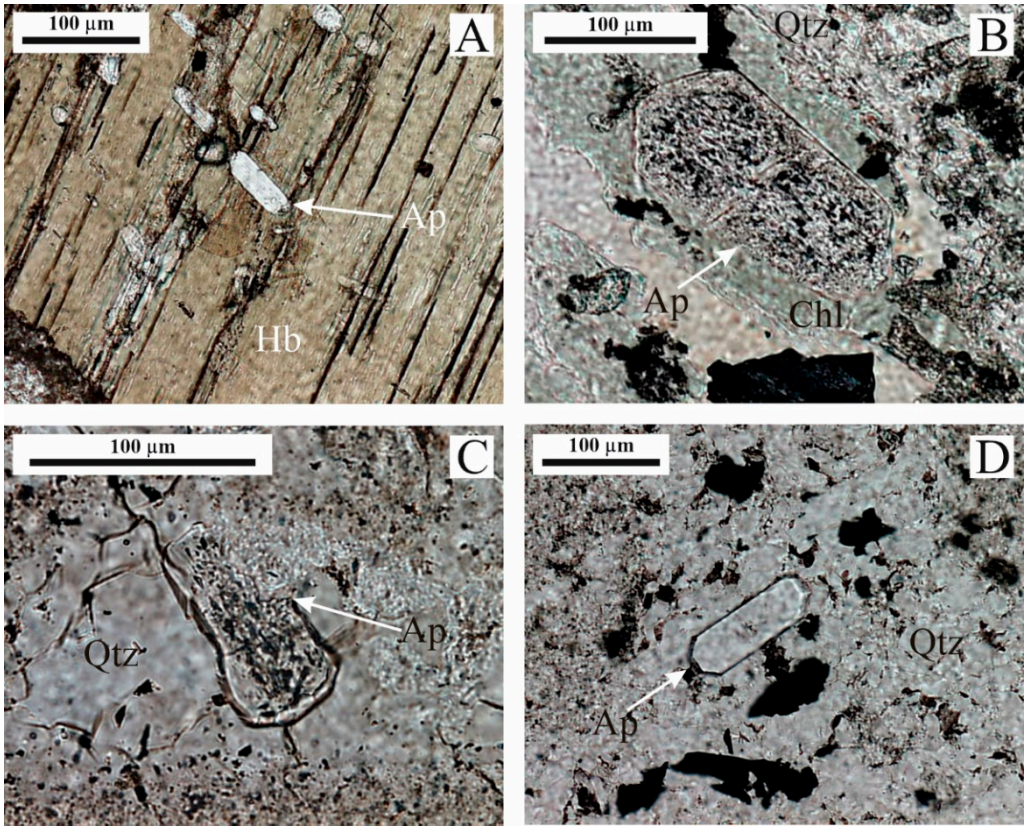

Figure 3. (**A**) Clean euhedral crystals of apatite (Ap) included in hornblende (Hb) in a calc-alkaline andesite from the vicinity of the Palai-Islica deposit. (**B**) Porous and corroded apatite (Ap) crystal inside a hornblende crystal replaced by chlorite (Chl) in a hydrothermally altered volcanic rock. (**C**) Porous and corroded apatite (Ap) in a quartz (Qtz) vein with sulfides. (**D**) Euhedral crystal of apatite without signs of corrosion in a quartz (Qtz) vein with sulfides.

In the hydrothermally altered volcanic rock, the apatite is also included in hornblende phenocrysts (Figure 3B) which have been transformed into a mixture of chlorite ± muscovite ± quartz ± dolomite. This kind of apatite appears porous and shows signs of corrosion (Figure 3B). The apatite in the orebody has been found as isolated crystals, with or without signs of corrosion (Figure 3C,D).

Apatite crystals of the four kinds were analyzed with a CAMECA SX50 electron microprobe ("Centro de Instrumentación Científica", University of Granada, Granada, Spain) using natural and synthetic standards. The operating conditions were 20 kV accelerating

potential, 20 nA beam current, and between 60 and 120 s X-ray peak and background acquisition times. The acquired X-ray intensities were corrected for atomic number, mass-absorption, and secondary fluorescence effects using the CAMECA-PAP version of the Pouchou and Pichoir procedure [41]. The results of these analyses, summarized in Table 1, indicate that there is significant variability in the apatite chemistry, mostly in halogen content. The compositions of apatite correspond to proportions of fluorapatite and chlorapatite ranging from 12% to 100% and from 0 to 57%, respectively. The proportion of hydroxylapatite calculated from stoichiometry ranges from 0 to 47% (Figure 4A,B). It should be noted that small quantities of Fe, Mg, and Mn have also been detected (Table 1).

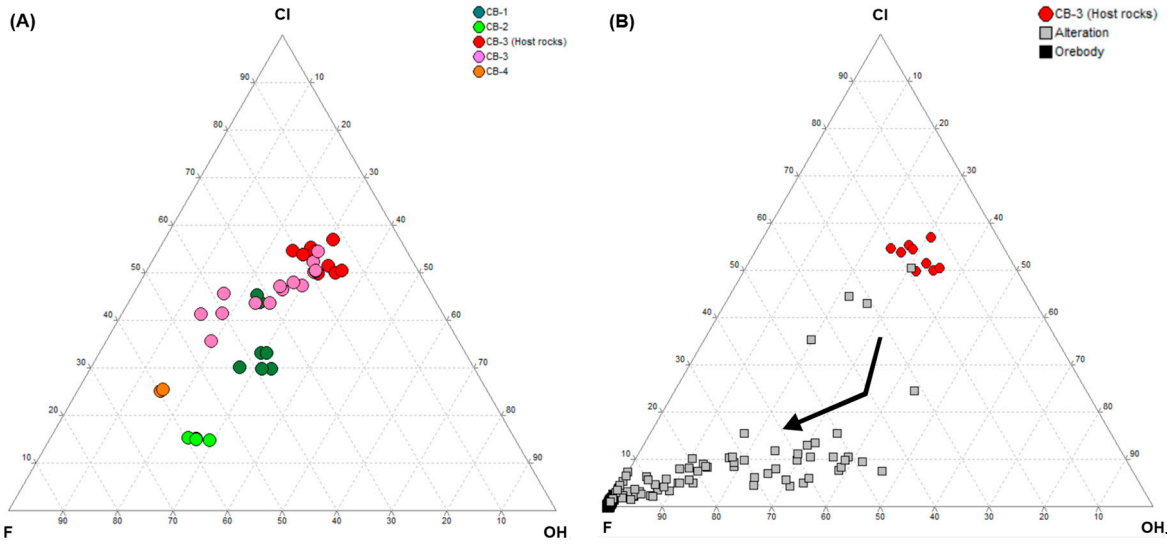

Figure 4. Cl-F-OH ternary diagram in mol units showing the chemistry of different types of apatite. (**A**) Apatites from volcanic rocks of different units: CB-1, CB-2, CB-3 (including both apatites from fresh calc-alkaline volcanic rocks hosting the mineralization and apatites from distal volcanic rocks), and CB-4. (**B**) Apatites from Palai-Islica deposit. CB-3 (host rocks): apatites from fresh calc-alkaline volcanic rock (CB-3 unit) hosting the mineralization. Alteration: apatites from hydrothermally altered volcanic rock. Orebody: apatites from quartz-veins with sulfides in the orebody.

The apatite in the volcanic rocks (CB-3 unit) hosting the Palai-Islica deposit has a relatively homogeneous composition, with the highest chlorapatite content (between 50% and 57%), the lowest fluorapatite content (between 12% and 21%), and intermediate hydroxylapatite content (between 24% and 36%) (Figure 4A). The concentration of Fe + Mg + Mn is the highest of all apatite analyzed (between 0.05 and 0.08 atoms per formula unit, a.p.f.u., Figure 5). Apatite from CB-3 far away from the deposit shows a slightly distinctive chemistry, shifted to more F-rich composition (Figure 4A).

Apatite in barren volcanic rocks from CB-1, CB-2, and CB-4 units, and distal volcanic rocks from CB-3, has a variable chlorapatite and fluorapatite composition (15–54% and 16–60%, respectively). The hydroxylapatite content ranges between 14% and 33% (Figure 4A).

The apatites from each unit show a distinctive composition. Thus, CB-3 shows the highest content of chlorapatite, while the apatite from the CB-2 unit shows the lowest of the volcanic samples.

Table 1. Chemistry of apatite crystals normalized to 13 O, OH, Cl, F.

	Volcanic Host Rocks (*n* = 9)				Other Volcanic Rocks (*n* = 28)				Hydrothermal Alteration (*n* = 80)				Orebody (*n* = 21)			
wt%	**Min**	**Max**	**Ave**	**s.d. (1s)**	**Min**	**Max**	**Ave**	**s.d. (1s)**	**Min**	**Max**	**Ave**	**s.d. (1s)**	**Min**	**Max**	**Ave**	**s.d. (1s)**
P_2O_5	41.44	42.87	41.90	0.46	41.11	42.73	42.23	0.35	40.20	43.28	42.24	0.58	40.08	41.89	41.00	0.57
FeO	0.39	0.63	0.51	0.08	0.43	1.28	0.78	0.23	0.00	0.53	0.15	0.12	0.00	0.12	0.04	0.04
MnO	0.09	0.16	0.12	0.02	0.04	0.15	0.10	0.03	0.00	0.13	0.06	0.03	0.00	0.12	0.05	0.03
MgO	0.12	0.20	0.15	0.03	0.08	0.33	0.18	0.07	0.00	0.42	0.03	0.06	0.00	0.05	0.00	0.01
SrO	0.00	0.09	0.04	0.03	0.00	0.00	0.00	0.00	0.00	0.17	0.04	0.04	0.00	0.08	0.02	0.02
CaO	53.77	54.49	54.14	0.22	52.64	54.60	53.86	0.40	52.69	56.46	55.26	0.76	53.59	55.81	54.97	0.55
F	0.46	0.78	0.62	0.09	0.61	2.24	1.38	0.52	0.71	4.35	2.93	0.78	3.46	4.62	4.27	0.25
Cl	3.47	4.02	3.69	0.19	1.03	3.79	2.63	0.86	0.08	3.51	0.59	0.63	0.00	0.18	0.07	0.06
Total	99.39	101.13	100.08	0.60	98.07	102.24	101.17	0.82	94.76	103.09	100.88	1.80	97.42	100.09	98.60	0.75
% fluorapatite	12	21	17	3	16	60	37	14	19	100	78	21	94	100	98	1
% chloroapatite	50	57	53	2	15	54	38	12	1	50	8	9	0	3	1	1
% hydroxylapatite	24	36	30	3	14	33	26	5	0	47	14	15	0	3	0	1
apfu																
P	2.99	3.04	3.01	0.01	3.00	3.04	3.02	0.01	2.97	3.02	3.00	0.01	2.95	3.02	2.98	0.02
Fe^{2+}	0.03	0.04	0.04	0.01	0.03	0.09	0.05	0.02	0.00	0.04	0.01	0.01	0.00	0.01	0.00	0.00
Mn^{2+}	0.01	0.01	0.01	0.00	0.00	0.01	0.01	0.00	0.00	0.01	0.00	0.00	0.00	0.01	0.00	0.00
Mg	0.01	0.02	0.02	0.00	0.01	0.04	0.02	0.01	0.00	0.05	0.00	0.01	0.00	0.01	0.00	0.00
Sr	0.00	0.00	0.00	0.00	0.00	0.00	0.00	0.00	0.00	0.01	0.00	0.00	0.00	0.00	0.00	0.00
Ca	4.83	4.96	4.92	0.04	4.82	4.92	4.87	0.02	4.89	5.06	4.97	0.03	4.95	5.12	5.05	0.05
F	0.12	0.21	0.17	0.03	0.16	0.60	0.37	0.14	0.19	1.13	0.78	0.21	0.94	1.26	1.16	0.07
Cl	0.50	0.57	0.53	0.02	0.15	0.54	0.38	0.12	0.01	0.50	0.08	0.09	0.00	0.03	0.01	0.01
OH	0.24	0.36	0.30	0.03	0.14	0.33	0.26	0.05	0.00	0.47	0.14	0.15	0.00	0.03	0.00	0.07

n: number of analysis; Min: minimum; Max: maximum; Ave: average; s.d.: standard deviation. Volcanic host rocks: apatites from fresh calc-alkaline volcanic rocks (CB-3 unit) that host Palai-Islica deposit. Other volcanic rocks: apatite from others volcanic units (CB-1, CB-2 and CB-4) and distal volcanic rocks from CB-3. Hydrothermal alteration: apatites from hydrothermally altered volcanic rock. Orebody: apatites from the mineralisation.

Apatite in the orebody has a relatively homogeneous composition, very different from that of the volcanic apatite, being almost pure fluorapatite (between 94% and 100%) with the lowest contents of chlorapatite (between 0 and 3%) and hydroxylapatite (between 0 and 3%) (Figure 4B). The concentration of Fe + Mg + Mn is always very low (between 0.00 and 0.01 a.p.f.u.) (Figure 5). This apatite shows the lowest values of Fe and Fe + Mg + Mn and the highest values of Ca (Figure 5A,B). It is noticeable that apatite can show bimodal chemical zonation, with sharp boundaries between dark rims and light cores in backscattered electron images (BSE; Figure 6A) that correlate with F-rich and F-poor composition, respectively. It is also remarkable that apatite in the Au enriched horizons is slightly richer in F (average difference of 0.07 a.p.f.u.).

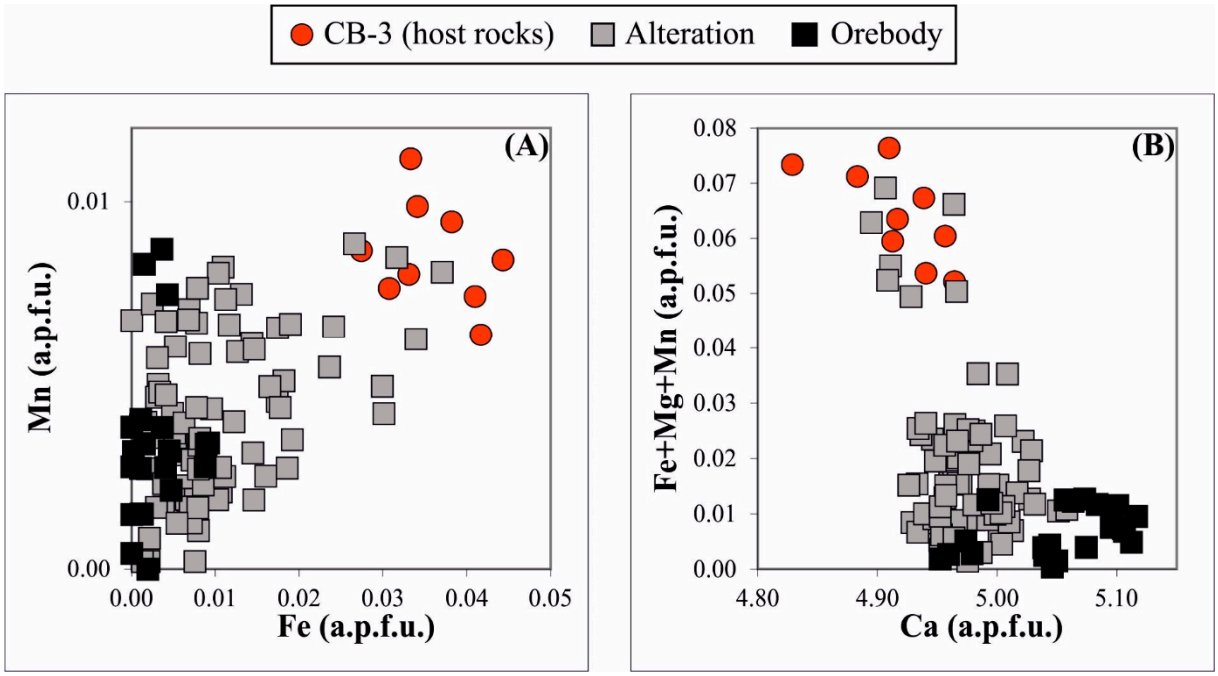

Figure 5. Binary diagrams of Fe vs. Mn (**A**) and Ca vs. Fe + Mg + Mn (**B**) of different types of apatite from Palai-Islica deposit. CB-3 (host rocks): apatites from fresh calc-alkaline volcanic rock (CB-3) hosting the mineralization. Alteration: apatites from hydrothermally altered volcanic rock. Orebody: apatites from quartz-veins with sulfides in the orebody.

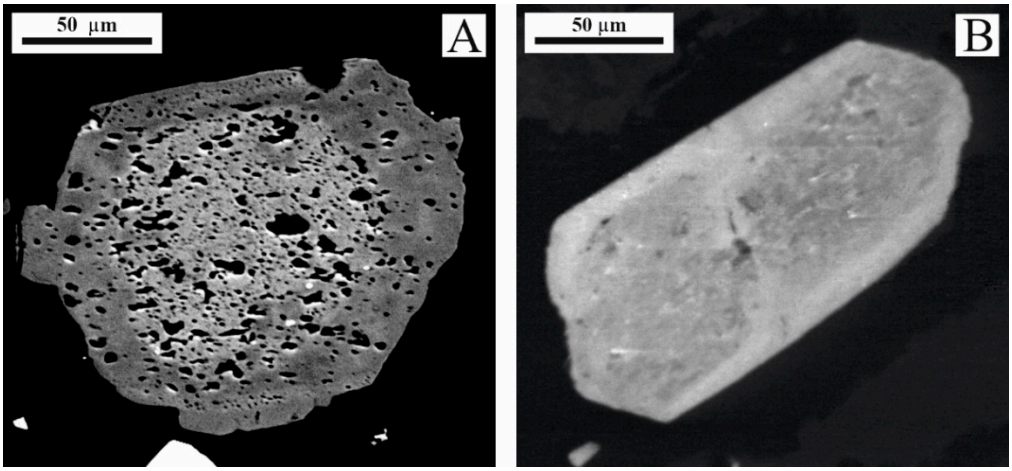

Figure 6. Backscattered electron image (BSE) of zoned apatite belonging to the mineralized veins (**A**) and to the hydrothermal alteration (**B**).

Apatite in the hydrothermally altered volcanic rocks (sericitic-chloritic and propylitic alteration) presents more variable compositions, with intermediate contents of fluorapatite (between 19% and 100%, average of 78%) and hydroxylapatite (between 0 and 47%, average of 14%). The chlorapatite (between 1% and 50%, average of 8%) component is also intermediate, although closer to the composition of apatite from the orebody (Figure 4B). The concentrations of trace elements such as Fe, Mg, and Mn are variable (Figure 5). These apatites show a zonation similar to that detected in the orebody, but also another one with dark cores and light rims in BSE (Figure 6B). Table 2 shows the core-rim compositional variations of individual apatite crystals, and a distinctive pattern could not be deduced.

Figure 7 shows the relationship between vertical distance with respect to the zone of intense mineralization, using the case of the Lower Geochemical Anomaly, and the chemistry of apatite from hydrothermal alteration. In this figure, the increase in F and decrease in Cl (and less significantly a decrease in Fe + Mg + Mn, and OH), with the proximity to LGA, is noticeable.

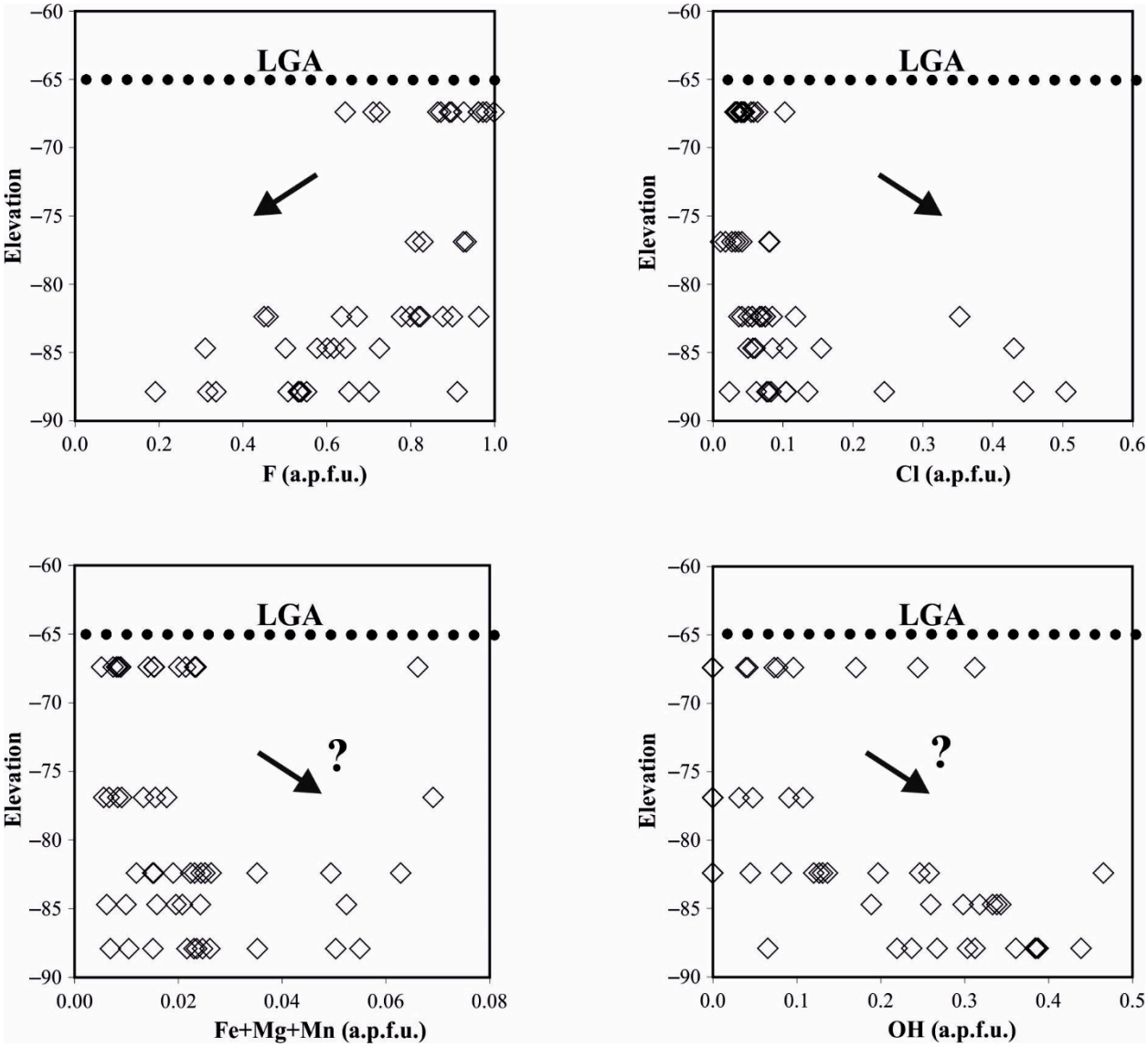

Figure 7. Diagrams showing the relationship between chemistry (F, Cl, Fe + Mg + Mn, and OH) of apatite crystals (diamonds) from the hydrothermal alteration and depth (elevation in meter above sea level). Diagrams include a dashed line indicating the position of the Lower Geochemical Anomaly (LGA). The arrow indicates the deduced trend in each diagram.

Table 2. Core-rim compositional variations of individual crystals of apatites from the hydrothermally altered volcanic rocks. Positive values indicate higher values in the core than in the rim.

Sample/Crystal	**S093/1**	**S108-1/1**	**S108-1/2**	**S108-1/3**	**S108-1/4**	**S109-1/1**	**S109-1/2**	**S109-1/3**	**S189-1/1**	**S189-1/2**	**S189-1/3**	**S189-1/4**	**S204/1**
Alteration Type	propylitic	sericitic-chloritic	sericitic-chloritic	sericitic-chloritic	sericitic-chloritic	sericitic-chloritic	sericitic-chloritic	sericitic-chloritic	propylitic	propylitic	propylitic	propylitic	sericitic-chloritic
F	−0.22	−0.19	0.05	0.15	−0.17	−0.03	0.05	0.05	0.42	0.35	−0.03	0.05	0.18
Cl	0.04	0.00	−0.05	−0.04	0.01	0.00	0.02	0.00	−0.03	−0.03	−0.01	0.03	−0.14
OH	0.18	0.19	0.00	−0.12	0.16	0.02	−0.07	−0.04	−0.38	−0.32	0.03	−0.08	−0.04
Fe + Mg + Mn	0.004	−0.007	0.015	−0.015	0.000	0.004	−0.003	0.000	−0.007	0.003	−0.005	−0.019	−0.017

4. Discussion

4.1. Origin of Apatite

From their textural characteristics, it can be deduced that apatite grains in the zones of hydrothermal alteration are inherited and not neoformed. Their chemistry suggests a chemical interaction of apatite grains with hydrothermal fluids. Thus, apatite is the only igneous phase, in addition to quartz and zircon, that is not destroyed by the action of the near-neutral hydrothermal fluids in the propylitic and sericitc-chloritic alteration. The acidic fluids related to the formation of argillic and advanced argillic alteration dissolve apatite crystals.

The apatite from the orebody has crystals with high porosity and corrosion features interpreted to be inherited from the volcanic rocks and mobilized by the hydrothermal fluids, which altered the rock, but clean crystals are neoformed. Although it seems that igneous apatite crystals were not completely dissolved, their composition was modified, as has been shown by the mineral chemical data.

4.2. Chemistry of Apatite Crystals and Their Evolution

The volcanic apatite from the Palai-Islica host rocks is rich in chlorapatite and hydroxylapatite components, with very low F content. This is surprising since magmatic apatite from other volcanic rocks in the area show more Cl and less F content than Palai-Islica host rocks. Even rocks from the same volcanic unit as the host rocks (CB-3), but outcropping several kilometers farther from the deposit, show slightly less Cl and more F content than host rocks (Figure 4A). Moreover, according to the literature, magmatic crystals are typically F-rich, Cl-poor (e.g., [11,42–44]). In apatites of granitoids from different localities, for example, Banks [3] found a maximum of 1.6 wt% of Cl, Teepper and Kuehner [9] found values that did not exceed 0.05 wt%, and Sha and Chappel [8] found a maximum of 0.7 wt% of Cl, which is very low compared with the range 3.47–4.02 wt% found in apatites in volcanic rocks that host the Palai-Islica deposit. Only in basic, less-fractionated rocks have high proportions of chlorapatite (up to 6.0 wt% of Cl in ultrabasic rocks [5]) been found. In addition, Piccoli and Candela [11], in a compilation of almost 1000 analyses in different types of magmatic apatite, found only one apatite belonging to felsic-intermediate rocks having a composition of Cl similar to the apatite of volcanic rocks related to the Palai-Islica deposit.

The Cl/F ratio of magmatic apatite is controlled by the differentiation processes (e.g., [4]), the formation of exsolved fluids (e.g., [45]), and the abundance of these elements in the magma source. The first two processes increase the F content in the apatite; therefore, the high Cl content of volcanic apatite from Cabo de Gata volcanism could be originated by the assimilation of Cl-bearing continental material by the magmas. These materials could be Triassic evaporites from the Betic Cordillera basement [30]. Moreover, enriched sulfur isotopic values for volcanic rocks in the Cabo de Gata–Cartagena belt (up to +7.3‰ [26]) and the enriched sulfur signature of different epithermal deposits with magmatic derived sulfur [26,40,46]) also suggest the incorporation in the magma of evaporites due to assimilation or contamination of the magmatic source. Geochemical and petrological studies of volcanic rocks of Cabo de Gata (e.g., [23,32]) also suggest assimilation processes. Furthermore, the local incorporation of these sulfur-bearing evaporites to the magma could be related to its potential fertility to produce sulfide-bearing ore deposits.

The apatites from the sericitic-chloritic and propylitic alteration, and, more so, those from the orebody, are rich in F. Other studies [47] that analyze both magmatic and hydrothermal related apatites do not show a fluorine enrichment in hydrothermal phases in respect to primary apatite, but just the opposite. Nevertheless, this fact occurs in different geological contexts in respect to the precious metal epithermal volcanic-hosted deposit of Palai-Islica, like REE-phosphate mineralization [47] or in a U volcanic-hosted hydrothermal deposit [48].

In the Palai-Islica deposit, the original volcanic apatite reacted with the hydrothermal fluids (in part, magmatic derived [29,39] and potentially F-bearing [49]), driving its composition to higher F content (and lower Cl, OH, and Fe + Mg + Mn contents). Since the ore-fluids and the fluids that produce the hydrothermal alteration are, essentially, the same fluids with complex and evolving physico-chemical characteristics, these modifications of the composition of apatite from hydrothermal alteration are directly related to the intensity of the alteration, that is, the fluid/rock ratios and the thermodynamic constrains. The chemistry of apatite from the hydrothermal alteration also suggests that the transformation of the original magmatic apatite favored the loss of Cl more than the loss of OH (Figure 4B).

These processes are more intense in the apatites from the orebody, and from the hydrothermal alteration near the Au-bearing horizons, with the formation, via transformation or direct crystallization, of apatite with a constant composition, with high F and very low Cl content, presumably buffered by the chemistry of the hydrothermal fluids.

The hydrothermal fluids are quite rich in Cl, as deduced from the fluid inclusions study (salinity is usually below 10% eq. NaCl, but can go up to 51.4% eq. NaCl, [29,39]), suggesting that the apatite/fluid partitioning coefficient at epithermal conditions must be very high for the case of F and, in comparison, very low for the case of Cl. Moreover, this has been experimentally demonstrated with apatite-fluid experiments at the 400–700 °C range [50]. Thus, fluorine partition coefficients of the apatite-fluid system are two orders of magnitude higher than apatite-melt in a magmatic system (higher coefficient at lowest experimental temperatures 400 °C). However, in the case of chlorine, this element shows a similar partition behavior in fluid and melt systems [50]. In this case, the zonation of apatite crystals in the orebody may be due to an extreme reaction and leaching of apatite, producing the lowest values of both Cl and OH.

Nevertheless, this behavior is only applicable in a near-neutral system. In strong acidic conditions, such as those associated with argillic and advanced argillic alteration, apatite was totally dissolved, not allowing apatite neoformation.

5. Conclusions

Apatite is a magmatic mineral, stable at a wide range of conditions, which typically does not disappear as a result of the action of near-neutral hydrothermal alteration. It has been shown to undergo significant modifications of its major-element composition through reactions with hydrothermal fluids, resulting in the production of F-rich apatites. This enrichment of F is related to the intensity of hydrothermal alteration and could thus constitute a geochemical index of alteration and geochemical exploration, the maximum F content in apatite coming from the orebody. This has been demonstrated by the case of the Palai-Islica deposit, where local anomalous Cl-rich volcanic apatites transformed into other F-rich apatites, almost without Cl, have been found.

Author Contributions: Conceptualization, J.C.-R. and S.M.-R.; methodology, J.C.-R. and S.M.-R.; sampling and data collection, J.C.-R., I.E.-A. and S.M.-R.; data analysis, J.C.-R. and S.M.-R.; interpretation data and discussion, J.C.-R., I.E.-A. and S.M.-R.; writing—original draft preparation, J.C.-R. and S.M.-R.; writing—review and editing, J.C.-R., I.E.-A. and S.M.-R.; funding acquisition, J.C.-R. and S.M.-R. All authors have read and agreed to the published version of the manuscript.

Funding: The research was initially supported by the Spanish projects BTE-2003-06265 and CGL2006-02594-BTE (Ministry of Science and Technology/Ministry of Science and Innovation/Ministry of Education and Science and FEDER), and the RNM 131 of Junta de Andalucía.

Data Availability Statement: Not applicable.

Acknowledgments: The authors thank Serrata Resources S.L. for the samples of the Palai-Islica deposit provided for this investigation. The authors also thank Juan Manuel Fernández Sóler (University of Granada) for his inestimable help with the selection of the samples of volcanic rocks and Antonio García Casco (University of Granada) for his constructive comments and criticism to the manuscript.

Conflicts of Interest: The authors declare no conflict of interest.

References

1. McConnell, D. *Apatite-Its Crystal Chemistry, Mineralogy, Utilization and Geological and Biological Occurrences*; Springer: Vienna, Austria; Heidelberg, Germany; New York, NY, USA, 1973; Volume 5, 111p.
2. Hughes, J.M.; Cameron, M.; Crowley, K.D. Structural variation in natural F, OH and Cl apatites. *Am. Mineral.* **1989**, *74*, 870–876.
3. Banks, N.G. Distribution of copper in biotite and biotite alteration products in intrusive rocks near two Arizona porphyry copper deposits. *U.S. Geol. Surv. J. Res.* **1974**, *2*, 195–211.
4. Nash, W.P. Phosphate minerals in terrestrial igneous and metamorphic rocks. In *Phosphate Minerals*; Nriagu, J.O., Moore, P.B., Eds.; Springer: Berlin, Germany; Heidelberg, Germany, 1984; pp. 215–241. [CrossRef]
5. Boudreau, A.E.; McCallum, I.S. Investigations of the Teilwater Complex: Part V. Apatites as indicators of evolving fluid composition. *Contrib. Mineral. Petrol.* **1989**, *102*, 138–153. [CrossRef]
6. Edgar, A.D. Barium- and strontium-enriched apatites in lamproites from West Kimberley, Western Australia. *Am. Mineral.* **1989**, *74*, 889–895.
7. Federico, M.; Peccerillo, A.; Barbieri, M.; Wu, T.W. Mineralogical and geochemical study of granular xenoliths from the Alban Hills volcano, Central Italy: Bearing on evolutionary proceses in potassic magma chambers. *Contrib. Mineral. Petrol.* **1994**, *115*, 384–401. [CrossRef]
8. Sha, L.K.; Chappell, B.W. Apatite chemical composition, determined by electron microprobe and laser-ablation inductively coupled plasma mass spectrometry, as a probe into granite petrogenesis. *Geochim. Cosmochim. Acta* **1999**, *63*, 3861–3881. [CrossRef]
9. Tepper, J.H.; Kuehner, S.M. Complex zoning in apatite from the Idaho batholith: A record of magma mixing and intracrystalline trace element diffusion. *Am. Mineral.* **1999**, *84*, 581–595. [CrossRef]
10. Belousova, E.A.; Griffin, W.L.; O'Reilly, S.Y.; Fisher, N.I. Apatite as an indicator mineral for mineral exploration: Trace-Element compositions and their relatonship to host rock type. *J. Geochim. Explor.* **2002**, *76*, 45–69. [CrossRef]
11. Piccoli, P.M.; Candela, P.A. Apatite in igneous systems. In *Phosphates: Geochemical, Geobiological and Material Importance*; Kohn, M.J., Rakovan, J., Hughes, J.M., Eds.; Mineralogical Society of America: Chantilly, VA, USA, 2002; Volume 48, pp. 255–292.
12. O'Sullivan, G.J.; Chew, D.M. The clastic record of a Wilson Cycle: Evidence from detrial apatite petrochronology of the Grampian-Taconic fore-arc. *Earth Planet. Sci. Lett.* **2020**, *552*, 116588. [CrossRef]
13. O'Sullivan, G.J.; Chew, D.M.; Morton, A.C.; Mark, C.; Henrichs, I.A. An integrated apatite geochronology and geochemistry tool for sedimentary provenance analysis. *Geochem. Geophys. Geosyst.* **2018**, *19*, 1309–1326. [CrossRef]
14. O'Sullivan, G.J.; Chew, D.M.; Kenny, G.; Henrichs, I.A.; Mulligan, D. The trace element composition of apatite and its application to detrital provenance studies. *Earth. Rev.* **2019**, *201*, 103044. [CrossRef]
15. Lu, J.; Chen, W.; Ying, Y.; Jiang, S.; Zhao, K. Apatite texture and trace element chemistry of carbonatite-related REE deposits in China: Implications for petrogenesis. *Lithos* **2021**, *398–399*, 106276. [CrossRef]
16. Knutson, C.; Peacor, D.R.; Kelly, W.C. Luminiscence, color and fission track zoning in apatite crystals of the Panasqueira tin-tungsten deposit, Beira-Baixa, Portugal. *Am. Mineral.* **1985**, *70*, 829–837.
17. Komninou, A.; Sverjensky, D.A. Hydrothermal alteration and the chemistry of ore-forming fluids in an unconformity-type uranium deposit. *Geochim. Cosmochim. Acta* **1995**, *59*, 2709–2723. [CrossRef]
18. Yang, F.; Chen, W.; Kynicky, J.; Ying, Y.; Bai, T. Combined in situ chemical and Sr isotopic compositions and U–Pb ages of the Mushgai Khudag Alkaline Complex: Implications of immiscibility, fractionation, and alteration. *Minerals* **2021**, *11*, 450. [CrossRef]
19. Chew, D.M.; O'Sullivan, G.; Caracciolo, L.; Mark, C.; Tyrrell, S. Sourcing the sand: Accessory mineral fertility, analytical and other biases in detrital U-Pb provenance analysis. *Earth Sci. Rev.* **2020**, *202*, 103093. [CrossRef]
20. Azizuki, M.; Nisidoh, H.; Kudoh, Y.; Watenabe, T.; Kurata, K. Sector growth and symmetry of (F,OH) apatite from the Asio Mine, Japan. *Mineral. Mag.* **1994**, *58*, 307–314. [CrossRef]
21. Mao, M.; Rukhlov, A.S.; Rowins, S.M.; Spence, J.; Coogan, L.A. Apatite Trace Element Compositions: A Robust New Tool for Mineral Exploration. *Econ. Geol.* **2016**, *111*, 1187–1222. [CrossRef]
22. Battistini, D.G.; Toscani, L.; Iaccarino, S.; Villa, I.M. K/Ar ages and the geological setting of calc-alkaline volcanics rocks from Sierra de Gata, SE Spain. *N. Jb. Miner. Mh.* **1987**, *8*, 337–383.
23. Turner, S.P.; Platt, J.P.; George, R.M.M.; Kelley, S.P.; Pearson, D.G.; Nowell, G.M. Magmatism associated with orogenic collapse of the Betic-Alboran domain, SE Spain. *J. Petrol.* **1999**, *40*, 1011–1036. [CrossRef]
24. Scotney, P.; Burgess, R.; Rutter, E.H. 40Ar/39Ar age of the Cabo de Gata volcanic series and displacements on the Carboneras fault zone, SE Spain. *J. Geol. Soc. London* **2000**, *157*, 1003–1008. [CrossRef]
25. López Ruiz, J.; Rodríguez Badiola, E. La región volcánica del SE España. *Estudios Geológicos* **1980**, *36*, 5–63.
26. Arribas, A.; Cunningham, C.G.; Rytuba, J.J.; Rye, R.O.; Kelly, W.C.; Podwysocki, M.H.; McKee, E.H.; Tosdal, R.M. Geology, geochronology, fluid inclusions, and isotope geochemistry of the Rodalquilar gold alunite deposit, Spain. *Econ. Geol.* **1995**, *90*, 795–822. [CrossRef]
27. Pineda Velasco, A. Las mineralizaciones metálicas y su contexto geológico en el área volcánica Neógena del Cabo de Gata (Almería, SE de España). *Boletín Geológico Minero* **1984**, *95*, 569–592.
28. Demoustier, A.; Castroviejo, R.; Charlet, J.M. Clasificación textural del cuarzo epitermal (Au-Ag) de relleno filoniano del área volcánica de Cabo de Gata, Almería. *Boletín Geológico y Minero* **1998**, *109*, 449–468.

29. Morales Ruano, S.; Carrillo Rosúa, F.J.; Fenoll Hach-Alí, P.; de la Fuente Chacón, F.; Contreras López, E. Epithermal Cu-Au mineralization in the Palai-Islica deposit, Almería, southeastern Spain: Fluid inclusion evidence of mixing of fluids as guide to gold mineralization. *Can. Mineral.* **2000**, *38*, 553–566. [CrossRef]
30. *Mapa Geológico de España. Escala 1:50,000 Hoja 1046 (24-42)*; Instituto Geológicoy Minero de España: Madrid, Spain, 1974.
31. Huibregtse, P.; van Alebeek, H.; Zaal, M.; Biermann, C. Paleostress analysis of the northern Nijar and southern Vera basins: Constraints for the Neogene displacement hystory of major strike-slip faults in the Betic Cordilleras, SE Spain. *Tectonophysics* **1998**, *300*, 79–101. [CrossRef]
32. Fernández Soler, J.M. El vulcanismo calco-alcalino en el Parque Natural de Cabo de Gata-Nijar (Almería). Estudio volcanológico y petrológico. Ph.D. Thesis, University of Granada, Granada, Spain, 1996; 295p.
33. Bellon, H.; Bordet, P.; Montenat, C. Chronologie du magmatisme Néogène des Cordillères Bètiques (Espagne mèridionale). *Bull. Soc. Géol. France* **1983**, *25*, 205–217. [CrossRef]
34. Carrillo-Rosúa, J.; Morales-Ruano, S.; Esteban-Arispe, I.; Fenoll Hach-Alí, P. Significance of phyllosilicate mineralogy and mineral chemistry in an epithermal environment. Insights from the Palai-Islica Au-Cu deposit (Almería, SE Spain). *Clays Clay Miner.* **2009**, *57*, 1–24. [CrossRef]
35. Carrillo-Rosúa, F.J.; Morales Ruano, S.; Fenoll Hach-Alí, P. The three generations of gold in the Palai-Islica epithermal deposit, southeastern Spain. *Can. Mineral.* **2002**, *40*, 1465–1481. [CrossRef]
36. Carrillo-Rosúa, F.J.; Morales-Ruano, S.; Fenoll Hach-Ali, P. Iron sulphides at the epithermal gold-copper deposit of Palai-Islica (Almería, SE Spain). *Mineral. Mag.* **2003**, *67*, 1059–1080. [CrossRef]
37. Carrillo-Rosúa, J.; Morales-Ruano, S.; Fenoll Hach-Alí, P. Textural and chemical features of sphalerite from the Palai-Islica deposit (SE Spain): Implications for ore genesis and color. *Neues Jahrb. Mineral. Abh.* **2008**, *185*, 63–78. [CrossRef]
38. Carrillo-Rosúa, J.; Morales-Ruano, S.; Roberts, S.; Morata, D.; Belmar, M. Application of the Mineralogy and Mineral Chemistry of Carbonates as a Genetic Tool in the Hydrothermal Environment. *Minerals* **2021**, *11*, 822. [CrossRef]
39. Carrillo Rosúa, F.J.; Morales Ruano, S.; Boyce, A.J.; Fallick, A.E. High and intermediate sulphidation environment in the same hydrothermal deposit: The example of Au-Cu Palai–Islica deposit, Carboneras (Almería). In *Mineral Exploration and Sustainable Development*; Eliopoulos, D.G., Ed.; Millpress: Rotterdam, The Netherlands, 2003; pp. 445–448.
40. Carrillo-Rosúa, J.; Esteban-Arispe, I.; Morales-Ruano, S.; Boyce, A.J.; Velasco, F. Epithermal volcanic-hosted deposits from SE Spain: Always derived from a magmatic sulfur source? *Geo-Temas* **2016**, *16*, 379–382.
41. Pouchou, J.L.; Pichoir, F. Un nouveau modèle de calcul pour la microanalyse quantitative per spectrométrie de rayons X. *La Reserche Aèrospatiale* **1984**, *3*, 167–192.
42. Deer, W.A.; Howie, R.A.; Zussman, J. *An Introduction to the Rock Forming Minerals*; Longman: Essex, UK, 1996; 540p.
43. Scott, J.A.J.; Humphreys, M.C.S.; Mather, T.A.; Pyle, D.M.; Stock, M.J. Insights into the behaviour of S, F, and Cl at Santiaguito Volcano, Guatemala, from apatite and glass. *Lithos* **2015**, *232*, 375–394. [CrossRef]
44. Kendall-Langley, L.A.; Kemp, A.I.S.; Hawkesworth, C.J.; EIMF; Roberts, M.P. Quantifying F and Cl concentrations in granitic melts from apatite inclusions in zircon. *Contrib. Mineral. Petrol.* **2021**, *176*, 58. [CrossRef]
45. Candela, P.A. Toward a thermodynamic model for the halogens in magmatic systems: An application to melt-vapor-apatite equilibria. *Chem. Geol.* **1986**, *57*, 289–301. [CrossRef]
46. Esteban-Arispe, I.; Velasco, F.; Boyce, A.J.; Morales-Ruano, S.; Yusta, I.; Carrillo-Rosúa, J. Unconventional non-magmatic sulfur source for the Mazarrón Zn–Pb–Cu–Ag–Fe epithermal deposit (SE Spain). *Ore Geol. Rev.* **2016**, *72*, 1102–1115. [CrossRef]
47. Andersson, S.S.; Wagner, T.; Jonsson, E.; Fusswinkel, T.; Whitehousee, M.J. Apatite as a tracer of the source, chemistry and evolution of ore-forming fluids: The case of the Olserum-Djupedal REE-phosphate mineralisation, SE Sweden. *Geochim. Cosmochim. Acta* **2019**, *255*, 163–187. [CrossRef]
48. Yu, Z.-Q.; Ling, H.-F.; Mavrogenes, J.; Chen, P.-R.; Chen, W.-F.; Fang, Q.-C. Metallogeny of the Zoujiashan uranium deposit in the Mesozoic Xiangshan volcanic-intrusive complex, southeast China: Insights from chemical compositions of hydrothermal apatite and metal elements of individual fluid inclusions. *Ore Geol. Rev.* **2019**, *113*, 103085. [CrossRef]
49. Sharma, R.; Srivastava, P.K. Hydrothermal Fluids of Magmatic Origin. In *Modelling of Magmatic and Allied Processes*; Kumar, S., Singh, R.N., Eds.; Society of Earth Scientists Series; Springer International Publishing: Cham, Switzerland, 2014; pp. 181–208. [CrossRef]
50. Kusebauch, C.; John, T.; Whitehouse, M.J.; Klemme, S.; Putnis, A. Distribution of halogens between fluid and apatite during fluid-mediated replacement processes. *Geochim. Cosmochim. Acta* **2015**, *170*, 225–246. [CrossRef]